

Cooperativity between *trans* and *cis* interactions in cadherin-mediated junction formation

Yinghao Wu^{a,b,d}, Xiangshu Jin^{a,b}, Oliver Harrison^{a,b}, Lawrence Shapiro^{a,b,c,1}, Barry H. Honig^{a,b,d,1}, and Avinoam Ben-Shaul^{e,1}

^aDepartment of Biochemistry and Molecular Biophysics, ^bHoward Hughes Medical Institute, and ^cEdward S. Harkness Eye Institute, Columbia University, New York, NY 10032; ^dCenter for Computational Biology and Bioinformatics, Columbia University, Room 815, 1130 St. Nicholas Avenue, New York, NY, 10032; and ^eInstitute of Chemistry and the Fritz Haber Research Center, Hebrew University, Jerusalem 91904, Israel

Contributed by Barry H. Honig, August 3, 2010 (sent for review June 8, 2010)

Intercellular junctions formed by cadherins, including desmosomes and adherens junctions, comprise two dimensional arrays of “*trans*” dimers formed between monomers emanating from opposing cell surfaces. Lateral “*cis*” interfaces between cadherins from the same cell surface have been proposed to play a role in cadherin clustering. Although the molecular details of *cis* interactions remain uncertain, they must define an anisotropic arrangement where binding is favorable only in certain orientations. Here we report Monte Carlo simulations performed on a 2D lattice constructed to account for the anisotropy in cadherin *cis* interactions. A crucial finding is that the “phase transition” between freely diffusing cadherin monomers and dimers and a condensed ordered 2D junction formed by dimers alone is a cooperative process involving both *trans* and *cis* interactions. Moreover, *cis* interactions, despite being too weak to be measured in solution, are critical to the formation of an ordered junction structure. We discuss these results in light of available experimental information on cadherin binding free energies that are transformed from their bulk solution values to interaction energies on a 2D lattice.

cis trans interfaces | cell adhesion | intercellular signaling

Cadherin-mediated cell–cell adhesion is initiated by the “*trans*” dimerization of cadherin monomers located on apposing cell surfaces (1–3). Binding triggers a series of still only partially understood cellular events that lead to the reorganization of the actin cytoskeleton that, in turn, trigger changes in cell morphology and motility (1–3). The formation of adherens junctions, whose core element consists of localized clusters of cadherins linked as adhesive dimers to cadherins from the apposed cell (4, 5), is likely to represent the first step in this signaling cascade. The interplay between *trans* binding and lateral (“*cis*”) interactions among proteins on the same membrane appears to play a crucial role in the clustering of cadherins into junctions. To elucidate the physical principles underlying this process, we present a theoretical model cast into a lattice-based Monte Carlo (MC) simulation scheme. Essential features of the model are derived from the 3D structures of cadherin ectodomains (6), and its implications are discussed in light of experimentally derived binding free energies (7). The coupling between *cis* and *trans* interactions appears to play a central role in cadherin-mediated cell–cell adhesion and may represent a general physical mechanism used in other adhesion processes as well.

Cadherins constitute a large Ca²⁺-dependent superfamily of cell surface adhesion receptors containing an N-terminal extracellular region, or ectodomain, followed by a single pass transmembrane segment and a C-terminal intracellular region that contains conserved binding sites for catenins (6, 8–10). The ectodomain of the type I cadherins, which are known to form junctions, consists of five tandem extracellular (EC) domains with immunoglobulin-like topology, ranging from the membrane-distal EC1 domain to the membrane-proximal EC5 domain (6) (Fig. 1). *Trans* dimerization is mediated by an interface formed between two cadherin molecules from opposing cells that swap the N-terminal β -strands of their EC1 domains, anchored

by binding of the highly conserved Trp2. Structural studies (6, 11–14), binding affinity measurements (7), sequence analysis (15), and molecular simulations (16, 17) have provided a detailed picture of the *trans* dimerization process that mediates cell-to-cell interaction.

A recent study has demonstrated that cadherin mutants lacking the cytoplasmic domain are capable of driving adherens junction formation, indicating that the structural determinants of this process reside in the ectodomain (18). The dense packing and apparent ordered structure of cadherins observed in EM and tomography studies of adherens junctions (19, 20) and desmosomes (21, 22) suggest the existence of lateral, *cis*, interactions between cadherin ectodomains positioned on the same cell surface. However, the location of the “*cis* interface” has not been conclusively identified. One possibility involves lateral contacts seen in the crystal structure of C-cadherin (2). This interface is formed in almost all cadherin ectodomain structures, providing evidence for its biological relevance. In the C-cadherin lattice, an interface is formed between the EC1 domain of one molecule and regions near the EC2–EC3 linker region in another (2, 6). These *cis* interactions produce a linear, one dimensional, array of cadherin ectodomains, as reflected in the lower layer of molecules in Fig. 1. In contrast, the cadherins shown in the upper layer are not in contact with each other but, rather, form similar linear arrays oriented along an out-of-plane axis with other cadherins from the same cell surface. Consequently, *trans* dimers interact with each other along two different directions, resulting in the production of a 2D lattice whose formation is driven by both *cis* and *trans* interactions. It is important to note that the strand-swapping *trans* interactions are weak compared to other dimer interactions with similar buried surface area (K_D s on the order of 20–100 μ M, corresponding to about 9–11 kT , k denoting Boltzmann constant and T the absolute temperature) (7). The *cis* interactions, which have not been observed in solution biophysical experiments, must be even weaker ($K_D > 1$ mM, i.e., about $7kT$). Yet the combination of the two is responsible for the formation of well-ordered junctions, consistent with recent single molecule studies that have provided direct evidence for the cooperativity between *cis* and *trans* interactions (23).

We approach the problem of adherens junction formation based on the premise that a junction can be described as an ordered 2D phase of densely packed *trans* dimers and simulate its formation using a lattice model inspired by the crystal structure of C-cadherin. Both the strand swapped *trans* interface and the newly defined *cis* interface are mapped onto a 2D lattice representing a superposition of the two adhering membranes.

Author contributions: Y.W., X.J., O.H., L.S., B.H.H., and A.B.-S. designed research; Y.W. performed research; Y.W., B.H.H., and A.B.-S. analyzed data; A.B.-S. contributed analytic tools; and Y.W., L.S., B.H.H., and A.B.-S. wrote the paper.

The authors declare no conflict of interest.

¹To whom correspondence may be addressed. E-mail: abs@fh.huji.ac.il, bh6@columbia.edu, or lss8@columbia.edu.

This article contains supporting information online at www.pnas.org/lookup/suppl/doi:10.1073/pnas.1011247107/-DCSupplemental.

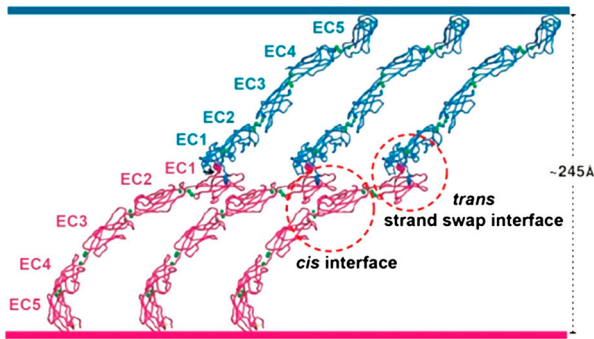


Fig. 1. *Trans* dimer organization, as derived from the crystal structure of C-cadherin (6).

MC simulations are carried out whereby cadherin monomers and dimers diffuse and interact via both *cis* and *trans* interactions, whose actual values may be estimated based on recent measurements of cadherin dimerization free energies in solution (7). We argue that lateral (*cis*) interaction between cadherin dimers, and/or monomers, can drive junction formation, provided their strength and the surface concentration are large enough.

There have been previous theoretical and lattice-based studies of clustering involving different types of adhesive proteins (24–29), including statistical-thermodynamic analyses of systems involving *cis* and *trans* interactions (26, 27), as well as various models of lateral receptor clustering (28, 29). However, none of these studies has been concerned with junction formation mediated by cadherins, nor with the special structural and energetic characteristics of these proteins and their crucial role in cell–cell junction formation. There are a number of other unique features to our present study. First, we introduce an experimentally informed anisotropic interaction scheme whereby directional intermolecular interactions are mapped onto a 2D lattice. A second important feature is the establishment of a connection between binding affinities measured in solution and the corresponding interaction energies to be used in the discrete quasi 2D lattice model. To this end, as originally suggested by Bell (24, 25), we define a quasi 3D “confinement shell” encompassing the midplane between the two membranes, within which the adhesive EC1 domains of cadherins from both membranes are assumed to freely diffuse and interact. We have previously used a related procedure in the description of the transient equilibrium established between *trans* interacting cadherins on apposing cell surfaces (30). Here we add directional *cis* and *trans* interactions to this model and map the confinement shell onto a 2D lattice, a procedure requiring a renormalization of the 3D measured binding energies.

Theory

Lattice Model. Although the adhesive interface of *trans* cadherin dimers is encompassed by the outermost (EC1) domain of the interacting monomers, the entire ectodomain plays an indirect, yet important, role in determining the probability of EC1–EC1 encounters. In the presence of Ca^{2+} ions, the ectodomains adopt a rigid “bow-like” structure, restraining EC1 fluctuations normal to the membrane plane to a relatively narrow shell of thickness h around the intermembrane midplane, as illustrated in Fig. 2. As in previous work (30) we assume that the EC1s from both membranes are uniformly distributed within this quasi 3D central shell.

To construct our lattice model we transcribe the central interaction shell of total area A into a 2D square lattice comprising M sites of area $a = A/M$. We associate a with the membrane area taken up by one cadherin molecule in a junction, estimated as the cross-sectional area of a single cadherin molecule in the C-cadherin crystal (6) ($a \approx 40 \text{ nm}^2$). We use A and B to denote the EC1

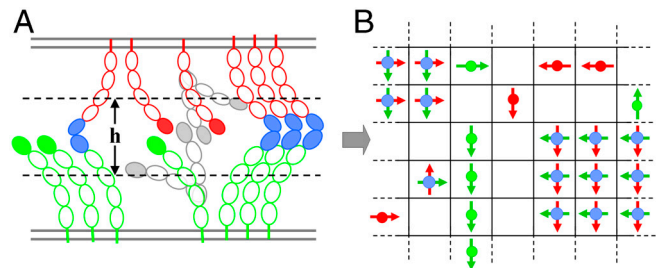


Fig. 2. (A) Schematic illustration of two interacting cadherin-decorated membranes. The EC1 domains are labeled by solid ellipses—green for cadherins in the lower membrane and red for those at the top layer. If apposed EC1 domains form a *trans* dimer they are labeled solid blue. Hollow ellipses label the EC2–EC5 domains. The gray “ghost” molecules illustrate alternative configurations, all within the interaction shell of thickness h . (B) The 2D square lattice, corresponding schematically to a top view on the interaction shell containing all EC1 domains, here depicted as dipoles (monomers). Each lattice site can accommodate no more than one top layer monomer (red dipole), nor more than one bottom layer monomer (green dipole). However, double occupancy by monomers belonging to apposed membranes is a necessary condition for *trans* dimer formation, provided the angle between the bottom and top monomers is 90° (indicated by a blue solid circle). The *cis* interactions between monomers and dimers are described in detail in the text.

domains of cadherin monomers originating in the top (A) and bottom (B) membranes, respectively, and $D = AB$ for the *trans* dimer formed in the binding reaction: $A + B \rightleftharpoons D$. The model does not allow double occupancy of one lattice site by two A s or two B s, thus accounting for excluded area interactions between nearest neighbor monomers. On the other hand, double occupancy by A and B is a necessary condition for *trans* dimer formation, implying that the volume element $ah \equiv \nu$ can accommodate the dimerized EC1s. We use Δg^0 (*trans*) to denote the free energy change, per dimer, in the dissociation process $D \rightarrow A + B$, i.e., Δg^0 (*trans*) > 0 if dimerization is energetically favorable.

As reflected by the crystal structure in Fig. 1 and schematically illustrated in Fig. 2A, the bow-like cadherin monomers form an ordered 1D aggregate, mediated by monomer–monomer contacts at the *cis* interface, whereby each molecule has exactly two nearest neighbors. *Trans* dimers, on the other hand, organize into 2D aggregates because their two constituent monomers each partake in *cis* interactions with 1D arrays of cadherins originating on apposed cell surfaces. Thus, in the crystal and, we propose, that in intercellular junctions as well, the two monomeric components of a *trans* dimer interact with monomers belonging to *different trans* dimers, as illustrated in Fig. 2B. In our “anisotropic” interaction model these properties are accounted for as follows. Monomers are treated as “dipoles” whose directions reflect the projection of their bent ectodomains onto the lattice plane. Dipoles may orient toward any of the four possible directions of the 2D square lattice, hereafter denoted as N , E , S , and W (for north, east, south, and west). Thus, there are four types of A monomers (dipoles) in our model, A_E , A_N , etc. in the top layer; B_E , B_N etc. in the bottom layer. Two monomers belonging to the same membrane interact with each other only if they occupy nearest neighbor sites along the same axis, e.g., a pair $A_N - A_N$ lying along the $S \rightarrow N$ axis. Thus, a monomer can interact (via its *cis* interface) with, at most, $z = 2$ nearest neighbors, which must be of the same kind. The *cis* interaction energy—corresponding to the free energy change upon the dissociation of a *cis* dimer is denoted as Δg^0 (*cis*), with Δg^0 (*cis*) ≥ 0 for attractive interactions.

Consistent with the crystal structure, we impose the condition that an A monomer can form a *trans* dimer only with a B monomer whose dipole is rotated clockwise by 90° , e.g., A_N can only bind to B_E yielding the *trans* dimer D_{NE} ($D_{NE} = A_N - B_E$). Because *cis* dimers can only form between monomers of the same orientation it follows that the two monomers of a given *trans* dimer must lie in different planes, as in the crystal. Owing to

the directionality of their constituent monomers, it follows that *trans*-dimers adhere only to nearest neighbor *trans*-dimers of the same kind (“chirality”), e.g., D_{NE} to D_{NE} . Assuming that dimer-dimer interactions are entirely due to the adhesive *cis* interfaces of their monomers, and that these are no different from those between isolated monomers, it follows that the interaction energy between neighboring *cis* dimers is also Δg^0 (*cis*). Note, however, that every *trans* dimer can interact with up to $z = 4$ other dimers, two via the *cis* interface of the monomers in the top layer A , and two with the orthogonally oriented monomers in the bottom layer, B . The nearest neighbor interaction energy between a properly oriented monomer-dimer pair (e.g., $A_N - D_{NE}$) is also Δg^0 (*cis*), and zero otherwise.

Monomers, for which $z = 2$, can self assemble into 1D aggregates along one of the four lattice directions. As is the general case for interacting particles in 1D, the average length of the aggregates is always finite (increasing with the total concentration of monomers and the attraction energy between them; see e.g., ref. 31). On the other hand, interacting particles in 2D—*trans* dimers in the present context—can undergo a first order phase transition to a macroscopic condensed phase, which we here interpret as a junction. The 1D oligomers of cadherin monomers are obviously more “fragile” than the 2D dimer islands. Thus, 1D oligomers may appear transiently in the system but are not expected to interfere with junction formation.

The total energy of the system, corresponding to a given distribution of monomers and dimers among the lattice sites, is given by

$$E = - \left[\sum_i (N_{A_i A_i} + N_{B_i B_i}) + \sum_k N_{D_k D_k} + \sum_k (N_{D_k A_{ki}} + N_{D_k B_{ki}}) \right] \Delta g^0(\text{cis}) - N_D \Delta g^0(\text{trans}) \quad [1]$$

where $N_{A_i A_i}$ is the number of $A_i - A_i$ pairs in the lattice, $i = N, E, S$, or W ; $N_{D_k D_k}$ is the number of $D_k - D_k$ dimers, with $k = NE, ES, SW$, or WN ; and $N_{D_k A_{ki}}$ denotes the number of adhesive contacts between dimers and A monomers, e.g., $D_{NE} - A_N$ etc. The last term in Eq. 1 is the sum of *trans* dimer energies, with $N_D = \sum_k N_{D_k}$. Note that the energy is measured relative to a reference state where all *cis* and all *trans* dimers are dissociated.

In our MC simulations whose results are reported in the following sections we use (Eq. 1) to calculate the energies of the various lattice configurations encountered in the course of a simulation run. The entropy of the system is automatically taken into account through the sampling of the many possible lattice configurations. Our goal in these simulations is to evaluate and characterize the strengths of *cis* and *trans* energies and the range of cadherin concentrations enabling the formation of thermodynamically and structurally stable junctions. Additional details about the simulation procedure are provided in *SI Text*.

From 3D Binding Affinities to 2D Lattice Energies. Binding free energies are derived in general from measurements of equilibrium concentrations in dilute 3D solutions. In *SI Text*, we relate the dissociation constant (K_D) measured in solution which is expressed in terms of 3D molar concentrations to κ_D , the corresponding dissociation constant on a lattice. In the lattice model, the membrane area is divided into M 2D cells of area a , and molecular concentrations are expressed in terms of the fractional lattice occupations $x_I \equiv N_I/M = N_I/(A/a) = \rho_I a$, where ρ_I is the 2D density of cadherin species I (either monomeric or dimeric) on the membrane surface; N_I denoting the total number of molecules of type I , and A is the membrane area. As before, we define Δg^0 as the free energy change, per molecule, when the dimer (either *cis* or *trans*) dissociates into monomers on the lattice. In *SI Text*

we show that the interaction energies of relevance in the lattice model, Δg^0 , and ΔG^0 , the corresponding molar binding free energies measured in 3D solution, are related by

$$\Delta g^0 = \Delta G^0/N_0 - kT \ln(ahN_0C_0) \quad [2]$$

where N_0 is Avogadro’s number and $C_0 = 1$ mole/liter is the unit molar concentration. We have previously estimated that $h \approx 10$ nm (30). Using, in addition, $a \approx 40$ nm², we find $ah \approx 400$ nm³ = 4×10^{-22} liter, implying that the numerical value of the second term in the last equation is approximately $5.5kT$. The physical reason underlying the lower magnitude of the lattice binding free energies as compared to those measured in bulk solution is that in solution the centers of mass of the molecules can translate continuously throughout space, whereas in the lattice they are clamped to lattice points. The translational entropy on the lattice is thus lower than in bulk solution, implying that in a dissociation process, where two translating particles are produced from one, the entropy gain on the lattice is smaller than that in bulk solution. The second term in Eq. 2 compensates for this lattice bias by reducing the magnitude of the binding free energy. This correction, like all the equilibrium constants above, is only valid in the dilute solution limit.

Numerical Results

We have carried out MC simulations for various combinations of initial concentrations and interaction parameters. The simulations were run typically for several hundred thousands MC steps until equilibrium has been reached or when the system is trapped in a metastable state that contains large but separate aggregates. In all systems considered the overall concentration of monomers in the two membranes (either as free monomers or dimerized) were set equal: $x_A^0 = x_B^0 \equiv x^0$ so that $x^0 = x_A + x_D = x_B + x_D$. The initial setup constitutes 100 cadherins distributed on each of the two-layer lattice sites. The lattices employed vary in size, between 25×25 to 100×100 sites, all with periodic boundary conditions, corresponding to three different overall monomer concentrations: 1%, 4%, and 16% ($x^0 = 0.01, 0.04$, and 0.16).

***Cis-trans* Coupling in Junction Formation.** Fig. 3 shows three simulation snapshots of the anisotropic model, all for the total concentration $x^0 = 0.16$. Fig. 3A describes a configuration of a system with strong *trans* binding ($\Delta g^0(\text{trans}) = 6kT$) but no *cis* interactions ($\Delta g^0(\text{cis}) = 0$). This system is an ideal 2D reactive

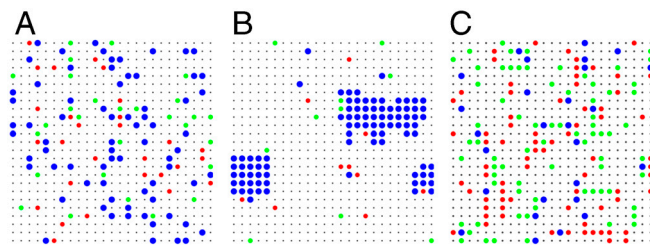


Fig. 3. Three simulation snapshots of the anisotropic lattice model. In all cases the overall monomer concentrations are 16% (i.e., $x_A^0 = x_B^0 \equiv x^0 = 0.16$). For clarity we use here a simpler notation, whereby red and green circles represent cadherins from the top and bottom membranes, and the larger, blue, circles denote *trans* dimers. (A) $\Delta g^0(\text{trans}) = 6kT$ and $\Delta g^0(\text{cis}) = 0$. The monomers and *trans*-dimers are in chemical equilibrium with each other, randomly dispersed among the lattice sites. (B) Both *cis* and *trans* interactions are sizeable: $\Delta g^0(\text{cis}) = 4kT$ and $\Delta g^0(\text{trans}) = 6kT$. The concentration of dimers is large enough and the lateral interaction between them strong enough to drive their condensation into well-defined ordered junctions. (C) *Trans* binding is weak, $\Delta g^0(\text{trans}) = 2kT$, and *cis* interactions are as large as in B, $\Delta g^0(\text{cis}) = 4kT$. The laterally attracting monomers aggregate into linear oligomers which in some cases involve the monomers belonging to *trans* dimers. The overall concentration of *trans* dimers is below the threshold concentration necessary for their 2D condensation into dimers.

($A + B \rightleftharpoons D$) mixture containing equilibrium proportions of monomers and dimers. Under these conditions of relatively high cadherin concentration and large *trans* binding energy most monomers associate into dimers: $x_D/x_A = x_D/x_B \approx 7/3 \approx 2.33$. No clustering of either dimers or monomers is noticeable, reflecting the absence of *cis* interactions.

Fig. 3B describes a system with the same *trans* binding energy as in Fig. 3A, $\Delta g^0(\text{trans}) = 6kT$, but the lateral interactions are also strong now, $\Delta g^0(\text{cis}) = 4kT$. The formation of cadherin-mediated junctions, manifested here as condensed islands of *trans* dimers, are clearly apparent, coexisting with a dilute “vapor” phase containing a small number of dimers in chemical equilibrium with a few monomers. Such equilibrium exists in principle in the condensed phase as well, except that the overall density there is so high that monomers cannot be seen. The overall number of dimers in the system of Fig. 3B is much larger than in Fig. 3A ($x_D/x^0 = 0.9$ vs. 0.7), most of them in the condensed phase, revealing that in addition to being necessary for inducing the formation of a junction, strong *cis* interactions also bias the monomer–dimer equilibrium in favor of the *trans* dimers. A final point regarding Fig. 3B is that the two large islands seen there correspond to two different dimer symmetries (*NE* vs. *SW*), each of which exhibits both translational and orientational order. Eventually, on a time scale much longer than that of our simulations, the two islands should coalesce into one. As in any simulation there are finite size effects in our system which, in the context of junction formation, are not unrealistic because of the limited number of cadherins in the system.

Finally, to demonstrate the coupling between *cis* and *trans* interactions in the system we show, in Fig. 3C, a simulation snapshot from a system where the *cis* interaction is the same as in Fig. 3B ($\Delta g^0(\text{cis}) = 4kT$), but the *trans* interaction is weaker than in the two previous snapshots: $\Delta g^0(\text{trans}) = 2kT$. No junctions (i.e., *trans* dimer islands) are seen now, despite the strong *cis* interaction. This is because the number of *trans* dimers in the system when $\Delta g^0(\text{trans}) = 2kT$ is low, below the threshold concentration for dimer condensation. Comparing Fig. 3B with Fig. 3C, we note that, for a given total concentration of cadherins in the system, there are certain threshold values of both the *cis* and the *trans* interactions, below which junction will not be formed. Moreover, these minimal *cis* and *trans* interactions are coupled to each other and depend on the overall protein concentration in the system, as discussed on a more quantitative basis in the following section.

The formation of a junction is, thermodynamically, a first order 2D phase transition that can only take place if the concentration of the interacting particles (*trans* dimers in our case) and the strength of the lateral interactions between them exceed certain threshold values. On the other hand, the aggregation of monomers is a 1D process, which can take place at any concentration and for any $\Delta g^0(\text{cis}) \geq 0$ *cis* interaction, yet it always results in the formation of linear oligomers of finite size. In analogy to other systems of linearly self-assembling particles, their average length can be shown to increase in proportion to the square root of the total concentration of monomers and exponentially with their adhesive energy (31). Linear arrays of *A* (red) and *B* (green) monomers are indeed seen in Fig. 3C, some of which involving also (the monomeric components of) *trans* dimers. Finally, it may be noted that if monomer–monomer interactions were isotropic rather than directional, i.e., taking place along all lattice directions ($z = 4$), they would tend to form uncorrelated 2D aggregates in the two monolayers, thus presenting a kinetic barrier to the formation of *trans* dimer junctions.

Phase Diagram. To evaluate the range of conditions favoring the formation of junctions we have carried out three series of MC simulations, corresponding to three different overall monomer concentrations ($x^0 = 0.01, 0.04, 0.16$). Each series consists of

several different combinations of $\Delta g^0(\text{trans})$ and $\Delta g^0(\text{cis})$, in order to examine whether a condensed phase has or has not been formed. Fig. 4 presents phase diagrams in the $\Delta g^0(\text{cis})$ vs. $\Delta g^0(\text{trans})$ plane, where each of the curves shown delineates the boundary between the mono-phase and two-phase regions corresponding to the given value of x^0 . Any point inside the enclosed area (at the bottom-right part) of the diagram lies within the two-phase region, where a junction phase coexists in equilibrium with a dilute vapor phase. For our present purposes, rather than using more rigorous statistical-thermodynamic methods to determine the phase boundaries (e.g., heat capacity changes), we sufficed here in a simpler approach and identified junction formation by the visual observation of well-defined dimer islands. Thus, for example, the curve in Fig. 4 corresponding to a total monomer concentration of 4% reveals that for a junction to form $\Delta g^0(\text{trans})$ must be at least $4kT$ and $\Delta g^0(\text{cis})$ must be larger than $5kT$. The mutual dependence of $\Delta g^0(\text{cis})$ and $\Delta g^0(\text{trans})$ along the phase boundary line is a direct reflection of the *cis*–*trans* coupling in determining the feasibility of junction formation. The figure reflects also the strong concentration dependence of the junction formation process.

Using MC simulations and approximate mean field solutions we have also analyzed the isotropic lattice model briefly mentioned earlier. Some of the predictions of this model are in qualitative agreement with the anisotropic models considered here, e.g., the phase diagrams exhibiting *cis*–*trans* coupling in junction formation.

It is clear from Fig. 4 that the predictions of the simulations depend on the values of the parameters used. We have determined the *trans* binding free energies in bulk solution for E- and N-cadherin as $\Delta g^0(\text{trans}) = 9$ and $11kT$, respectively, corresponding (using the approximately $5.5kT$ lattice correction from Eq. 2) to between about 3.5 and $5.5kT$, (7). According to Fig. 4, these values are, roughly, in the range allowing junctions to form, provided $\Delta g^0(\text{cis})$ is no less than about $4kT$. Steinberg and coworkers (32) have produced cell lines with expression levels ranging from about 25,000 to 250,000 molecules per cell which, for 10 μm diameter cells, correspond to values of x^0 ranging between about 0.01 to 0.1. Thus, the phase diagrams shown in Fig. 4 present results for concentration ranges that are physically meaningful. More detailed theoretical and computational analyses are now in progress, relating the *cis* and *trans* binding energies of cadherins in 3D solution to those prevailing in the quasi 2D adhesive interface between two cells. A somewhat related problem involving the association of integral membrane proteins has been treated previously (33).

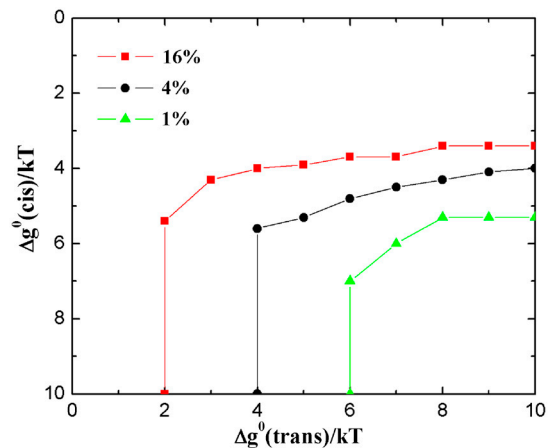


Fig. 4. Phase boundaries between the dilute one-phase region (left and above each curve) and the two-phase region, marking the appearance of a condensed junction phase consisting of *trans*-dimers.

The Diffusion Trap Mechanism. In general, upon initial cell–cell contact, the adhesive region between two cells is considerably smaller than their total area. That is, membrane curvature effects would be expected to prevent most cadherins from reaching one another, except in the contact zone. In such cases the cadherins tend to diffuse from distal regions to the contact zone, enhancing the concentration in the contact zone and depleting the distal ones. There have been previous theoretical treatments of related phenomena reported in the literature for other systems (34, 35). This process, with the contact zone serving as a “diffusion trap” (36, 37), takes place even in the absence of lateral interactions.

To visualize the role of the diffusion trap we show in Fig. 5 two simulation snapshots of a system consisting of 50×50 lattice sites, containing a central contact zone—the trap—comprising 10×10 lattice sites, surrounded by a wide belt of lattice sites representing the region of large intermembrane separation. In these simulations *A* and *B* monomers diffuse anywhere on the lattice but *trans* dimer formation can only take place in the contact zone. Two systems are contrasted in Fig. 5, both with the same average total concentration (4%) and the same *trans* binding energy ($\Delta g^0(\text{trans}) = 6kT$), with $\Delta g^0(\text{cis}) = 0$ in Fig. 5*A* vs. $\Delta g^0(\text{cis}) = 4kT$ in Fig. 5*B*. As expected, the total concentration in the trap is enriched even in the absence of lateral attraction; from 4% to about 15% in Fig. 5*A*, with most monomers associated into—randomly scattered—*trans* dimers. A dramatically different behavior, both qualitatively and quantitatively, is exhibited when *cis* interactions are turned on, as shown in Fig. 5*B*. The lateral interactions are now strong enough to drive most of the cadherins ($\sim 80\%$) into the contact zone, which constitutes just a small region (4%) of the total area, corresponding to enrichment by a factor of 20, as compared to 3.5 in Fig. 5*A*. Moreover, within the trap, practically all cadherins condense into an ordered, tightly packed, junction of *trans* dimers. Note also that if the contact zone were simply the entire membrane area, then for the same *cis* and *trans* energies and overall concentration (4%) considered in Fig. 5*B*, we conclude from Fig. 4 that under these conditions a junction will not form because the point $\Delta g^0(\text{trans}) = 6kT$, $\Delta g^0(\text{cis}) = 4kT$ lies outside the two-phase region. It is the dramatic buildup of molecules in the contact zone combined with the synergetic roles of *trans* dimerization and *cis* mediate aggregation that drives junction formation.

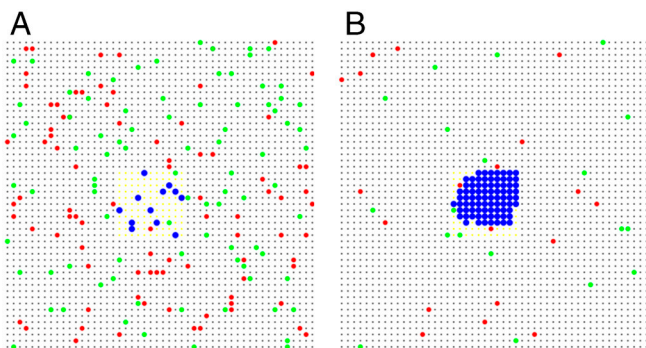


Fig. 5. A diffusion trap comprising 10×10 lattice sites in the center of a 2D lattice of 50×50 sites, with periodic boundary conditions. *Trans* dimer formation can only take place in the central zone—the trap. The distance between membranes in the surrounding region is too large to allow *trans* dimer formation. In both snapshots shown, $\Delta g^0(\text{trans}) = 6kT$ and the average monomer density is $x^0 = 0.04$. The trap area is 4% of the total area. (A) No lateral attraction between monomers and/or dimers, $\Delta g^0(\text{cis}) = 0$. After equilibration the overall concentration in the trap increases to nearly 14%. (B) Here, $\Delta g^0(\text{cis}) = 4kT$. Monomers migrate into the trap where they dimerize, enriching the *trans* dimer population in the trap. The strongly attracting dimers condense into an ordered island attracting additional cadherin molecules into the trap. The higher concentration of cadherins in the trap enhances their dimerization, while the strong *cis* binding encourages their lateral condensation into a junction.

Discussion

Our primary goal in this work has been to present a mechanism explaining how junctions can be formed from cadherin molecules that undergo *trans* interactions with other cadherins on opposing cells and *cis* interactions with molecules on the same cell. Our basic hypothesis has been that a junction comprises an ordered 2D lattice that can be viewed as a thermodynamically condensed phase of *trans*-dimers, held together by attractive *cis* interactions. An anisotropic lattice model has been constructed with *cis* interactions based on crystallographic evidence that identifies a distinct lateral adhesive interface between neighboring molecules (6). However, it is important to emphasize that the results presented here are not dependent on the fine structure of the model but, rather, represent general properties of at least some adhesion receptors. Specifically, if there is only one lateral interface formed between two receptor proteins, this can only lead to a linear (1D) array of molecules, as seen for example in a single layer of C-cadherin crystal lattice, or in the linear array formed by unliganded ephrin receptors (38). In contrast, for cadherins, the formation of an adhesive *trans* dimer provides two sets of lateral interactions that are oriented in different directions, thus allowing for the formation of a 2D lattice.

A key result of the model is that junction formation is a cooperative process involving both *trans* and *cis* interactions. In the absence of *cis* interactions, *trans* dimers would be formed but no ordered structure would be observed. Localization of monomers in a contact zone through a diffusion trap mechanism substantially enhances *trans* dimer formation, but a junction will not be formed in the absence of lateral *cis* interactions of sufficient magnitude. Moreover, there may be upper limits to the strength of *trans* interactions determined by the requirement that cell–cell adhesive strengths be relatively weak upon initial cell–cell contact (e.g., prior to junction formation) (30). On the other hand, the phase diagrams in Fig. 4 show that there is a concentration dependent lower limit for $\Delta g^0(\text{trans})$ below which no junction will form, independent of the magnitude of $\Delta g^0(\text{cis})$.

Additional constraints involve the strength of *cis* interactions. Specifically, because receptor clustering initiates a variety of downstream signaling events, it is essential that lateral interactions are not large enough to drive the clustering of cadherin monomers in the absence of cell–cell contact. This of course is not a problem if *cis* interactions are weak, yet as argued above, they must be strong enough to drive junction formation. How can both requirements be met? One possibility is that *cis* interactions are weak in monomers and strong in dimers. Because there is nothing preventing the putative monomer interface to be identical to that observed in dimers, differences in the strength of *cis* interactions in monomers and dimers could only be realized through a mechanism not involving the interface itself. In this work we have assumed that the strength of *cis* interactions is identical for the monomer and dimer and, nevertheless, clustering is only observed for the dimer. This is a consequence of the fact, mentioned above, that 1D interactions cannot drive a first order phase transition. Short monomer oligomers could potentially be formed when *cis* interactions are large enough, but their aggregation into a condensed 2D phase is not possible. *Trans* dimers, in contrast, are structured so as to allow the formation of an ordered 2D lattice.

The relationship between cadherin binding free energies in bulk (3D) solution, and the corresponding (2D) binding free energies when the cadherins are bound to lipid membranes is complex. We estimated the interaction energies used in the lattice model based on an approximate model for the quasi 2D interaction zone between the adhering cells. The question of deducing 2D binding free energies from 3D measurements extends far beyond the use of a lattice model. In the absence of direct measurements of 2D energies, a theory addressing this issue is both important and challenging. Such theory should, for instance,

take into account the different amplitudes of EC1 fluctuations along the membrane normal in the monomer vs. *trans* dimer states, the role of membrane fluctuations, and the different numbers and characters of the translational and internal (rotational and vibrational) degrees of freedom of the interacting cadherins in 2D vs 3D. A detailed study addressing these issues is underway.

The results presented in this work are not intended to present a quantitative picture of the energetic basis of adherens junction formation, but rather to describe the physical principles that underlie this process. To summarize, we begin with the widely accepted premise that the initial recognition event upon cell–cell contact involves the formation of *trans*-dimers between cadherin monomers located on apposing surfaces. *Cis* interactions then mediate the clustering of these dimers into ordered structures that correspond to junctions. We have argued that junction formation is a cooperative process involving both *cis* and *trans* interactions; *trans* dimers form in the absence of *cis* interactions but their number is increased, as does the overall adhesive strength, when a transition to an ordered condensed phase is enabled by the existence of *cis* interactions with a well-defined directionality. Moreover, since it is essential that downstream signaling not occur in the absence of cell–cell contact, the system must be designed so as to avoid lateral clustering in the absence

of *trans* dimerization. This is ensured by the fact that *cis* interactions are weak and by the structure of cadherin monomers that can only form 1D aggregates, whereas cadherin dimers can form ordered 2D structures.

Although we have focused here on cadherins, it is worth noting that receptor clustering is a prevalent mechanism of intercellular signaling, observed for example in the formation of the immunological synapse (39, 40) and in ephrin-mediated cell–cell interactions (41, 42). Although the molecular details that characterize each of these systems are quite different, the basic principles are likely to be related to those discussed here. Indeed, as mentioned above, a recent report of the crystal structure of ephrin A and its receptor (38) reveals a combination of functionally important *cis* and *trans* interactions in the crystal lattice that is quite similar to those discussed here.

ACKNOWLEDGMENTS. We thank Orly Slavin, Izhar Medalsi, and Sergey Troyanovsky for helpful discussions. This work was supported by National Science Foundation Grant MCB-0918535 (to B.H.H.) and National Institutes of Health Grant R01 GM062270-07 (to L.S.). The financial support of the US-Israel Binational Science Foundation (Grant 2006-401, to A.B.-S., B.H., and L.S.) and the Israel Science Foundation (Grant 659/06 to A.B.-S) is gratefully acknowledged.

- Troyanovsky S (2005) Cadherin dimers in cell-cell adhesion. *Eur J Cell Biol* 84:225–233.
- Shapiro L, Weis WI (2009) Structure and biochemistry of cadherins and catenins. *Cold Spring Harbor Perspect Biol* 1:a003053.
- Halbleib JM, Nelson WJ (2006) Cadherins in development: Cell adhesion, sorting, and tissue morphogenesis. *Genes Dev* 20:3199–3214.
- Yap AS, Briehner WM, Gumbiner BM (1997) Molecular and functional analysis of cadherin-based adherens junctions. *Annu Rev Cell Dev Biol* 13:119–146.
- van Roy F, Bex G (2008) The cell-cell adhesion molecule E-cadherin. *Cell Mol Life Sci* 65:3756–3788.
- Boggon TJ, et al. (2002) C-cadherin ectodomain structure and implications for cell adhesion mechanisms. *Science* 296:1308–1313.
- Katsamba P, et al. (2009) Linking molecular affinity and cellular specificity in cadherin-mediated adhesion. *Proc Natl Acad Sci USA* 106:11594–11599.
- Patel SD, Chen CP, Bahna F, Honig B, Shapiro L (2003) Cadherin-mediated cell-cell adhesion: Sticking together as a family. *Curr Opin Struct Biol* 13:690–698.
- Yamada S, Pokutta S, Drees F, Weis WI, Nelson WJ (2005) Deconstructing the cadherin-catenin-actin complex. *Cell* 123:889–901.
- Weis WI, Nelson WJ (2006) Re-solving the cadherin-catenin-actin conundrum. *J Biol Chem* 281:35593–35597.
- Overduin M, et al. (1995) Solution structure of the epithelial cadherin domain responsible for selective cell adhesion. *Science* 267:386–389.
- Parisini E, Higgins JM, Liu JH, Brenner MB, Wang JH (2007) The crystal structure of human E-cadherin domains 1 and 2, and comparison with other cadherins in the context of adhesion mechanism. *J Mol Biol* 373:401–411.
- Haussinger D, et al. (2004) Proteolytic E-cadherin activation followed by solution NMR and X-ray crystallography. *EMBO J* 23:1699–1708.
- Patel SD, et al. (2006) Type II cadherin ectodomain structures: Implications for classical cadherin specificity. *Cell* 124:1255–1268.
- Posy S, Shapiro L, Honig B (2008) Sequence and structural determinants of strand swapping in cadherin domains: Do all cadherins bind through the same adhesive interface? *J Mol Biol* 378:954–968.
- Cailliez F, Lavery R (2006) Dynamics and stability of E-cadherin dimers. *Biophys J* 91:3964–3971.
- Sotomayor M, Schulten K (2008) The allosteric role of the Ca²⁺ switch in adhesion and elasticity of C-cadherin. *Biophys J* 94:4621–4633.
- Hong S, Troyanovsky RB, Troyanovsky SM (2010) Spontaneous assembly and active disassembly balance adherens junction homeostasis. *Proc Natl Acad Sci USA* 107:3528–3533.
- Farquhar MG, Palade GE (1963) Junctional complexes in various epithelia. *J Cell Biol* 17:375–412.
- McNutt NS (1970) Ultrastructure of intercellular junctions in adult and developing cardiac muscle. *Am J Cardiol* 25:169–183.
- He WZ, Cowin P, Stokes DL (2003) Untangling desmosomal knots with electron tomography. *Science* 302:109–113.
- Al-Amoudi A, Diez DC, Betts MJ, Frangakis AS (2007) The molecular architecture of cadherins in native epidermal desmosomes. *Nature* 450:832–837.
- Zhang Y, Sivasankar S, Nelson WJ, Chu S (2009) Resolving cadherin interactions and binding cooperativity at the single-molecule level. *Proc Natl Acad Sci USA* 106:109–114.
- Bell GI (1978) Models for the specific adhesion of cells to cells. *Science* 200:618–627.
- Bell GI, Dembo M, Bongrand P (1984) Cell adhesion. Competition between nonspecific repulsion and specific bonding. *Biophys J* 45:1051–1064.
- Weikl TR, Lipowsky R (2001) Adhesion-induced phase behavior of multicomponent membranes. *Phys Rev E* 64:011903.
- Weikl TR, Asfaw M, Kroboth H, Rozycki B, Lipowsky R (2009) Adhesion of membranes via receptor-ligand complexes: Domain formation, binding cooperativity, and active processes. *Soft Matter* 5:3213–3224.
- Sackmann E (2006) Thermo-elasticity and adhesion as regulators of cell membrane architecture and function. *J Phys-Condens Mat* 18:R785–R825.
- Reister-Gottfried E, et al. (2008) Dynamics of specific vesicle-substrate adhesion: From local events to global dynamics. *Phys Rev Lett* 208103.
- Chen CP, Posy S, Ben-Shaul A, Shapiro L, Honig BH (2005) Specificity of cell-cell adhesion by classical cadherins: Critical role for low-affinity dimerization through beta-strand swapping. *Proc Natl Acad Sci USA* 102:8531–8536.
- Ben-Shaul A, Gelbart WM (1994) *Micelles, Membranes, Microemulsions and Monolayers* (Spinger, New York).
- Foty RA, Steinberg MS (2005) The differential adhesion hypothesis: A direct evaluation. *Dev Biol* 278:255–263.
- Grasberger B, Minton AP, Delisi C, Metzger H (1986) Interaction between proteins localized in membranes. *Proc Natl Acad Sci USA* 83:6258–6262.
- Qi SY, Groves JT, Chakraborty AK (2001) Synaptic pattern formation during cellular recognition. *Proc Natl Acad Sci USA* 98:6548–6553.
- Komura S, Andelman D (2000) Adhesion-induced lateral phase separation in membranes. *Eur Phys J E* 3:259–271.
- Troyanovsky RB, Laur O, Troyanovsky SM (2007) Stable and unstable cadherin dimers: Mechanisms of formation and roles in cell adhesion. *Mol Biol Cell* 18:4343–4352.
- Perez TD, Tamada M, Sheetz MP, Nelson WJ (2008) Immediate-early signaling induced by E-cadherin engagement and adhesion. *J Biol Chem* 283:5014–5022.
- Seiradake EH, Sutton G, Aricescu AR, Jones EY (2010) An extracellular steric seeding mechanism for Eph-ephrin signaling platform assembly. *Nat Struct Mol Biol* 17:398–402.
- Dustin ML (2009) Multiscale analysis of T cell activation: Correlating in vitro and in vivo analysis of the immunological synapse. *Visualizing Immunity, Current Topics in Microbiology and Immunology* (Springer-Verlag Berlin, Berlin), 334, pp 47–70.
- Fooksman DR, et al. (2010) Functional anatomy of T cell activation and synapse formation. *Annu Rev Immunol* 28:79–105.
- Pasquale EB (2008) Eph-ephrin bidirectional signaling in physiology and disease. *Cell* 133:38–52.
- Himanen JP, Saha N, Nikolov DB (2007) Cell-cell signaling via Eph receptors and ephrins. *Curr Opin Cell Biol* 19:534–542.